JOURNAL OF THE KOREAN ASTRONOMICAL SOCIETY
36: S101 ~ S107, 2003

PROPAGATION OF SUDDEN IMPULSES IN A DIPOLAR MAGNETOSPHERE

DONG-HUN LEE AND SUK-KYUNG SUNG
Department of Astronomy & Space Science and Institute of Natural Sciences
Kyung Hee University, Yongin, Kyunggi, 449-701, Korea
E-mail: dhlee@khu.ac.kr

ABSTRACT

The magnetosphere is often perturbed by impulsive input such as interplanetary shocks and solar wind discontinuities. We study how these initial perturbations are propagating within the magnetosphere over various latitude regions by adopting a three-dimensional numerical dipole model. We examine the wave propagation on a meridional plane in a time-dependent manner and compare the numerical results with multi-satellite and ground observations. The dipole model is used to represent the plasmasphere and magnetosphere with a realistic Alfven speed profile. It is found that the effects of refraction, which result from magnetic field curvature and inhomogeneous Alfven speed, are found to become important near the plasmapause. Our results show that, when the disturbances are assumed at the subsolar point of the dayside magnetosphere, the travel time becomes smaller to the polar ionosphere compared to the equatorial ionosphere.

Key words : Magnetosphere, Sudden Commencement, Magnetic Storm

I. INTRODUCTION

Interplanetary shocks and solar wind discontinuities can give rise to relatively large-scale perturbations in the magnetosphere. These impacts at the dayside magnetopause, which cause storm sudden commencements(SSC) and sudden impulses(SI), are expected to launch sudden perturbations into the magnetosphere. Hydromagnetic waves have often been adapted to describe the propagation of SSC and SI in the magnetosphere since several decades ago (e.g., Francis et al. 1959; Wilson & Sugiura 1961; Nishida 1964 ; Stegelmann & von Kenschitzki 1964; Tamao 1964; Burlaga & Ogilvie 1969). The SSC events are usually followed by geomagnetic storms and accompanied by southward interplanetary magnetic fields, which do not appear with the SI events. However, the leading edge of both SSC and SI in the magnetosphere is represented by relatively sharp wavefront, which propagates with the Alfven speed. Thus, sudden impulses(SI) will be used in this paper to include both cases.

While compressional impulses propagate into the magnetosphere across magnetic shells, they continuously produce transverse waves via mode conversion by inhomogeneity and/or curved geometry (Hasegawa et al. 1983). Thus polarization and amplitude as well as arrival times based on any local measurements are expected to strongly depend on wave coupling and dipolar geometry in the magnetosphere (Lee & Lysak 1999). Recently, investigations of the propagation of SI have been emphasized since compressional pulses are known to play an important role in the energization of radiation belt electrons and protons (e.g., Li et al. 1993 ; Hudson et al. 1995, 1996).

Magnetic perturbations arriving at the surface of the Earth become significantly affected by the existence of the ionosphere. Kikuchi and Araki (1979a, 1979b) studied the ionospheric responses associated with the sudden impulses by assuming the Earth-ionosphere waveguide system. The onset time distributions and their observational characteristics were investigated and well summarized by Araki (1977, 1994).

The spatial and temporal structures of SI have been investigated by a number of observations on ground-based magnetometers and satellite measurements(e.g., Nopper et al. 1982; Wilken et al. 1982; Knott et al. 1985; Wedeken et al. 1986; Petrinec et al. 1996; Araki et al. 1997). However, most of previous work has not revealed the details of SI propagation on its way from the outer space to the ionosphere. It is partly due to the facts that (1) a limited number of satellites are not capable of tracing the propagation of disturbances in a highly refractive system such as the magnetosphere, and (2) ground-based measurements such as magnetometers are allowed to see only secondary signals which are modified and reproduced by the ionosphere.

Recently, Lee & Kim (2000) and Lee & Hudson (2001) studied the propagation properties in a three-dimensional dipole model. These numerical experiments showed that the leading edge of SI undergoes strong refraction owing to inhomogeneous Alfven speed in a dipolar magnetosphere. The travel time between the equatorial magnetopause and the polar ionosphere is found to be shorter than that between the magnetopause and the deep plasmasphere. In this paper, in order to study more details of SI propagation in the magnetosphere, we will introduce and discuss the ob-

Corresponding Author: D.-H. Lee

servational characteristics based on the previous studies. We will also present a case study of multi-satellite and ground observational data from recent SI events, which strongly support the results of the numerical experiments.

II. MODEL AND NUMERICAL RESULTS

This numerical experiment is based on the recent three-dimensional dipole model (Lee & Hudson 2001) which adopted different boundary conditions at different local times. The inner boundary is at $L = 2$ and the outer boundary is at $L = 10.5$, and perfect reflecting boundary conditions are used at the ionospheres, which are assumed to be at an altitude of 0.5 R_E, where R_E represents the Earth's radius. We apply different boundary conditions at the dayside and nightside outer regions, respectively. At the dayside magnetopause the Alfven speed drops from $V_{\rm ms} = 600$ km/s in the magnetosphere to $V_{\rm sw} = 60$ km/s in the solar wind. Thus the reflection coefficient at the dayside boundary is given by $r = V_{\rm ms} - V_{\rm sw}/V_{\rm ms} + V_{\rm sw}$ when waves are propagating out of the magnetosphere. With this boundary condition, wave energy can escape from the magnetosphere across the dayside magnetopause. In the nightside region, we assume a free boundary condition, that there is no reflection from the nightside magnetosphere (Lee & Hudson 2001).

The two linearized wave equations in a cold plasma are given by

$$(\vec{\nabla} \times \vec{B})_\perp = \frac{1}{{V_A}^2}\frac{\partial \vec{E}}{\partial t} \quad (1)$$

$$\vec{\nabla} \times \vec{E} = -\frac{\partial \vec{B}}{\partial t}, \quad (2)$$

where V_A is the Alfven speed. These equations are solved by a leapfrog scheme (Lee & Lysak 1989) in the dipole coordinates $(\hat{\mu}, \hat{\nu}, \hat{\phi})$ similar to those used by Chen & Hasegawa (1974). Thus $\hat{\nu}$ is normal to the field line pointing outward, and $\hat{\phi}$ is the usual azimuthal direction $(\hat{\mu} = \hat{\nu} \times \hat{\phi})$. The grid points are $98 \times 98 \times 98$ points along each coordinate. The model boundaries are referred to Lee & Hudson (2001). The Alfven speed profile used in this study is shown in Figure 1.

We assume a propagating impulse at the dayside magnetopause. This impulse is given by E_ϕ which corresponds to a radial compression. Disturbances are assumed to be symmetric in both latitude and local time and the size of an impulse is assumed to be about 5 R_E x 10 R_E in each direction at the dayside magnetopause. We have investigated time histories at various locations. A set of grid points has been selected across the magnetic shells near the equatorial region and the polar region slightly above the ionosphere, respectively.

Figure 2 shows the time histories of the magnetic electric fields at the dayside equatorial region. In Figure 2, the impulse is propagating across the equatorial magnetic shells, which are evident in the compressional components (B_μ, B_ν, E_ϕ). The transverse components (B_ϕ, E_ν) stay quiet since they have nodes at the equator due to the symmetry of the initial impulse. The wave propagation becomes slower inside the plasmasphere $(L < 6)$ owing to the relatively small Alfven speed. It takes $t = 70$ s until the signal reaches the inner magnetic shell near $L = 2.4$. In the dayside polar region, Figure 3 shows that the earliest signals are found around $t = 40$ in all components, which indicates that the travel time from the subsolar point to the polar region can be shorter than that to the deep plasmasphere near the equator. Thus effects of refraction are very large in the magnetosphere in the sense that the geometric path between the source and the inner plasmasphere is shorter than that between the source and the polar ionosphere, which is consistent with the previous numerical studies (Lee & Kim 2000). It is interesting to note in Figure 3 that the compressional components almost simultaneously arrive in the polar region except for part of the plasmaspheric region, while the transverse components become differentiated in latitude. In the transverse components in Figure 3, the earliest signals are found near $L = 6$ where the Alfven speed become largest in the magnetosphere. This feature can be explained by the wave coupling between the compressional and transverse waves. When the initial impulse propagate radially inward from the magnetopause, transverse waves are continuously excited and start propagating along each field line.

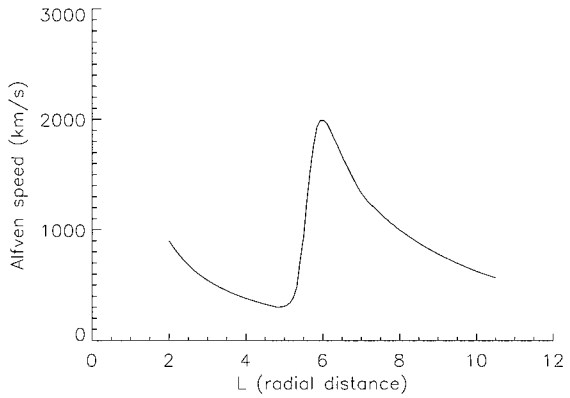

Fig. 1.— The equatorial Alfven speed profile assumed in this model.

Our results suggest that the path of the least travel time to the polar ionospheric region is along the magnetic field line located near the outer edge of the plasmapause where the Alfven speed is largest in the outer magnetosphere. For higher latitudes, the wavefronts become slightly delayed. Compressional components in Figure 3 are sensitive not to the direction of the magnetic field, but to the magnitude, which is associated with the Alfven speed. Thus the travel paths

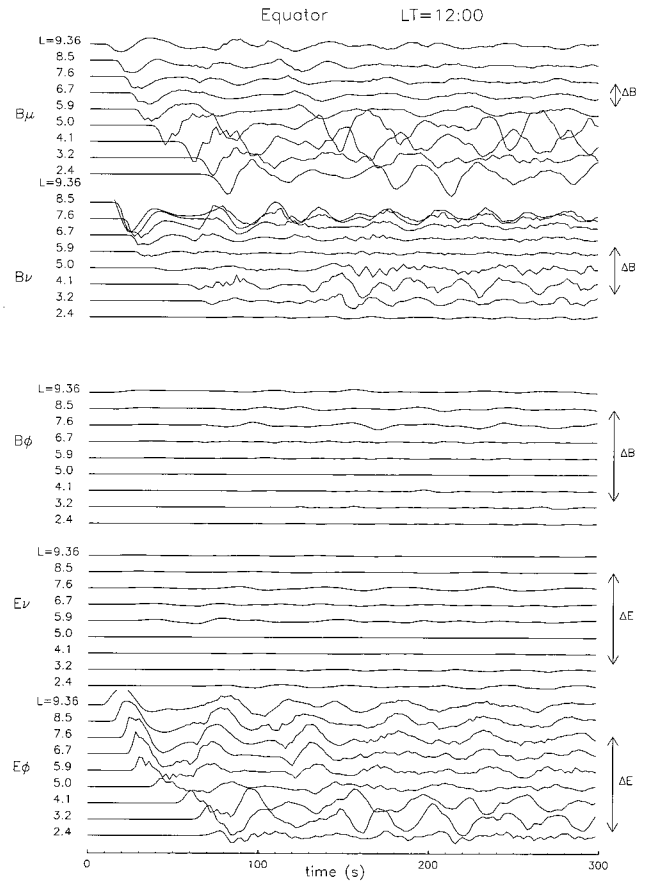

Fig. 2.— Time histories of the magnetic and electric fields at the equatorial region.

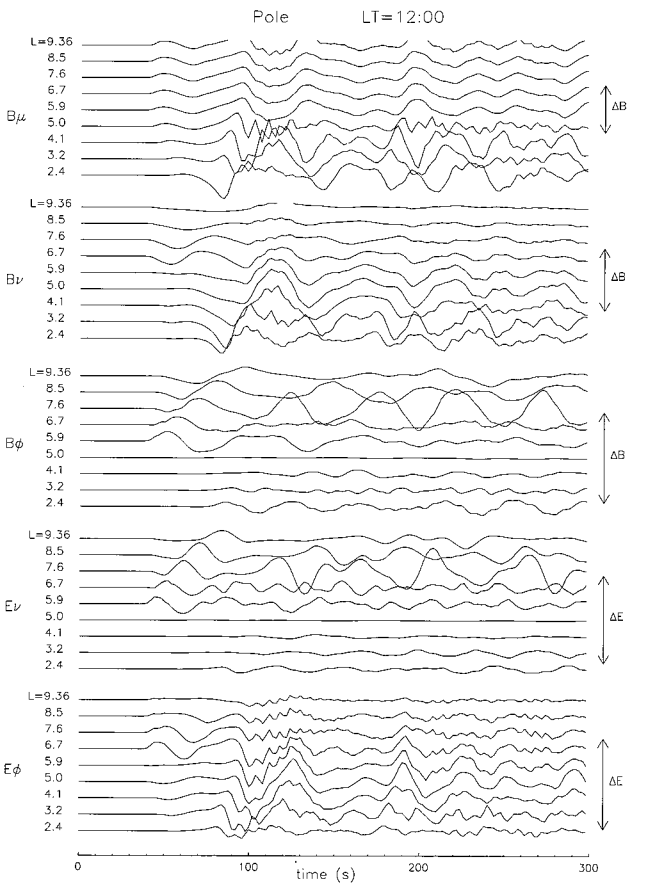

Fig. 3.— Time histories of the magnetic and electric fields at the polar region.

become independent of the field lines and the arriving signals are almost in phase over different latitudes in the polar region except for the deep plasmasphere. On the other hand, the transverse waves in the polar region have phase shifts at different latitudes since they are guided along different field lines. It is interesting to note that the leading edges of B_ϕ and E_ν in Figure 3 show polarization reversals near $L = 6.7$ in addition to the continuous phase shifts in arrival times.

III. OBSERVATIONS

Near UT 0400 on September 3, 2000, the earth's magnetosphere was suddenly perturbed. This event is observed by 3 satellites and a number of ground stations. As shown in Figure 4, this is a single pulse event which is suitable to compare with the numerical experiments. Figure 4 shows the magnetic field data of the ACE, WIND and GEOTAIL. All three satellites were located in the solar wind, and their position were shown in Figure 5. At 0305 UT(A), the ACE spacecraft at 235 R_E upstream of the Earth observed that total magnitude and z component of magnetic fields suddenly dropped during 6 minutes. Other satellites observed the same feature. The WIND observed the magnetic field variations at 0342 UT(B), and GEOTAIL observed at 0407 UT(C), respectively. In the numerical experiment, the impulse propagates at the dayside magnetopause. To determine the area that the shockfront becomes encounter the magnetopause, we assume two hypotheses. One is that the velocity and direction of the SI are almost constant in the solar wind. The other is ignoring the variations in z direction. Time intervals T1 and T2 in Figure 4 are 35 min and 25 min. And in Figure 5, the top panel is $x - y$ plane and the bottom is $x - z$ plane in GSE coordinates. Since the distances among three satellites in z are relatively small, it is expected that this shockfront can be examined only on $x - y$ plane. Using each distance and time interval, we obtain the SI velocity and its propagating direction. The velocity is about 452.93 km/sec and the SI arrive point is near 1600 local time.

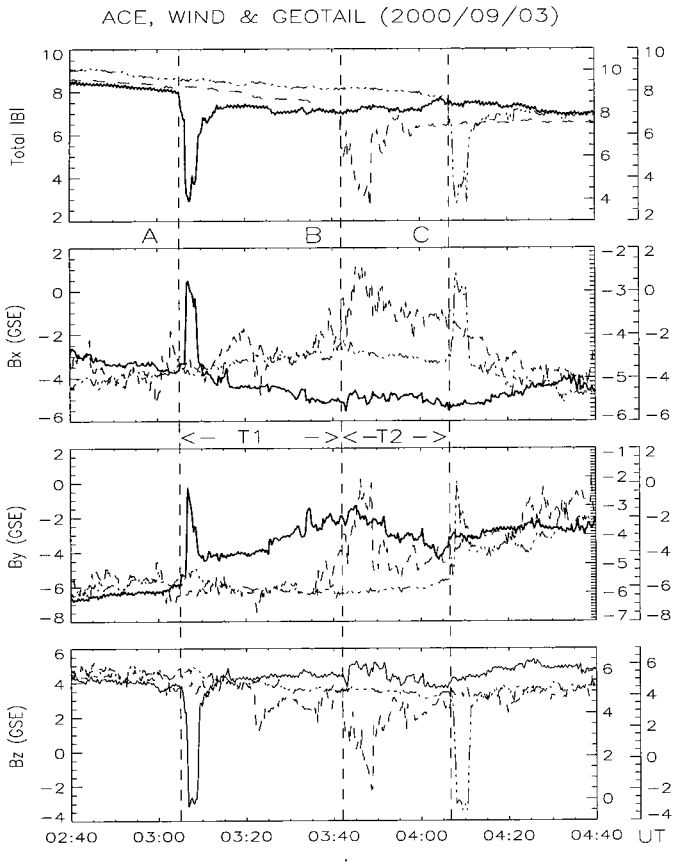

Fig. 4.— Magnetic field data from ACE, WIND, and GEOTAIL. The thick line represents the ACE magnetic field data and the dashed and dash-dot lines represent the WIND and GEOTAIL data, respectively.

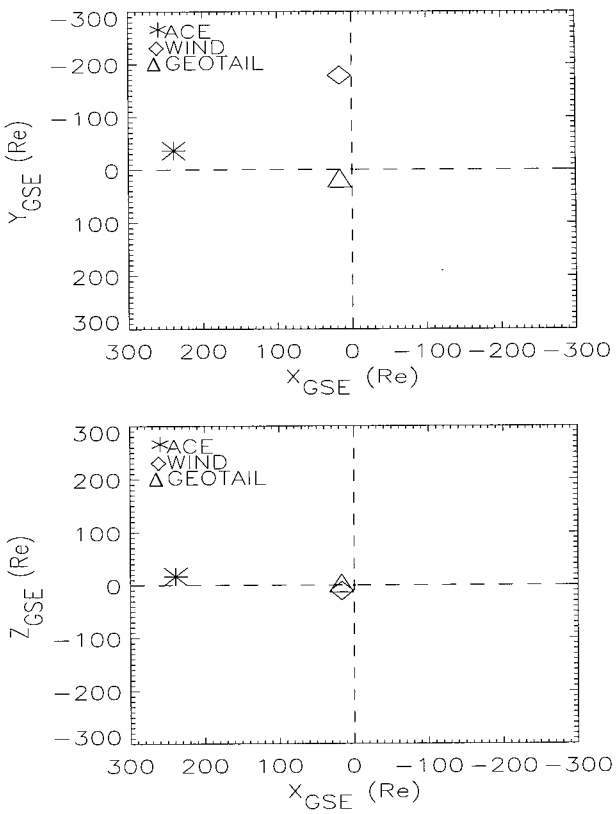

Fig. 5.— The positions of 3 satellites in GSE coordinates. An oblique line represent the shock front.

(a) Ground Station Magnetometer

There are a large number of stations in the five geomagnetic networks International Monitor for Auroral Geomagnetic Effects (IMAGE), Sub-Auroral Magnetometer Network (SAMNET), 210° Magnetic Meridian (210MM), Geophysical Institute Magnetometer Array (GIMA), Canadian Auroral Network for the Open Program Unified Study (CANOPUS)) for this event. We have plotted in Figure 6 the H-component for 66 ground stations for 15 minutes surrounding the onset time. At UT 0405 IMAGE and SAMNET is located on a little prenoon side of the impact region. And 210MM is located on the dusk side. GIMA and CANOPUS are located on the nightside. General features are as follows: Within the morning side auroral zone(IMAGE and SAMNET), a positive pulse precedes a negative pulse. Contrarily, within the afternoon and night side(210MM, GIMA and CANOPUS), a negative pulse precedes a positive pulse. In addition, the preliminary reverse impulse(PRI) is distinctly seen in the afternoon sector(210MM). And 210MM data is qualitatively similar to the input single pulse, while the other ground station data show oscillatory fluctuations after the wavefront.

To verify the wavefront delay near the polar region, we select some stations along the magnetic latitude in each network(Table 1). These stations are located along the almost same magnetic longitude. Area 1, which consists of 8 IMAGE stations, is close to the impact region of the shock front. Their magnetic longitudes are 56.89° - 75.25°, and the longitudes are 102.18° - 112.08°. Figure 7 shows a plot of the variations of the H component of the geomagnetic field observed by IMAGE. In this Figure, the stations are listed according to the magnetic latitude. The amplitudes is found to become larger as the latitude increases (NAL to BJN stations). To obtain the arrival sequence, we compared two adjacent station data(Figure 8). Although, we cannot obtain the exact time difference, this superposition is useful to distinguish the preceding one from the following one. Figure 7 and Figure 8 indicates that the earliest signal is found near SOD station in Area 1. Its magnetic latitude is 63.92 °. Similarly, it is found that HLL(64.69°), GAK(63.54°) and

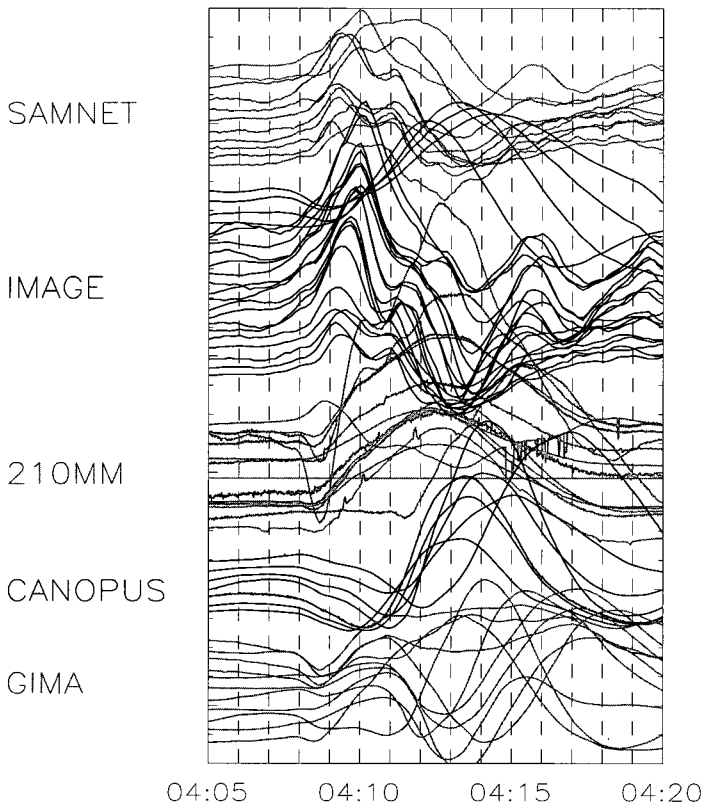

Fig. 6.— H component from 66 ground stations.

GILL(63.88°) stations observed the earliest signal in Area 2, 4, and 5, respectively. The stations in Area 3 are located mid and low latitude and it is very difficult to distinguish the arrival time sequence over latitudes. However in any cases, the fastest signal is observed near 63° - 65° magnetic latitude.

The effect of SI on the magnetosphere can be understood either from a mechanical or an electrodynamical point of view (Lysak et al. 1994). From a mechanical point of view, while the leading edge of SI propagates away in the antisunward direction, the input at the magnetopause causes the boundary motion, which consists of a radially inward velocity followed by a radially outward velocity later on. The inward velocity region first occurs at the initial contact point, which is expected to move down to the antisunward direction, in which Figure 9 shows such an illustrative example. In this inward region, the magnetic field is compressed, leading to an enhancement of the magnetic pressure which diverts the flow to both sides azimuthally. Similarly, in the region of outward(recovering) flow the magnetic pressure decreases, which draws the flow in azimuthally. Thus, the flow between the inward and outward velocity regions is driven azimuthally toward

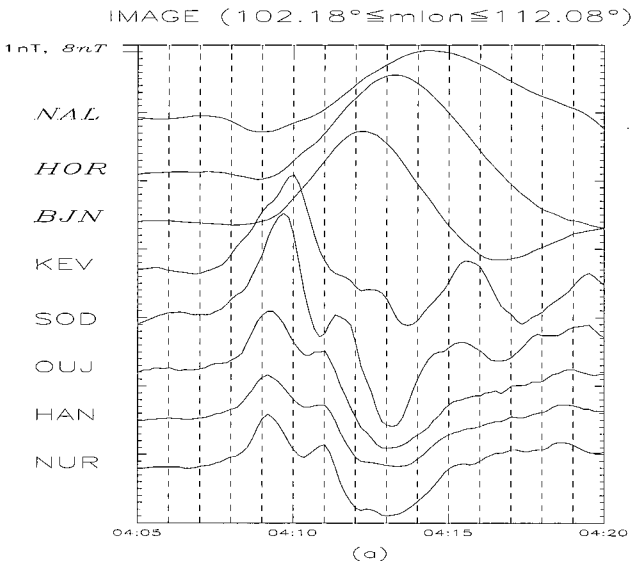

Fig. 7.— H component from 8 stations in IMAGE network.

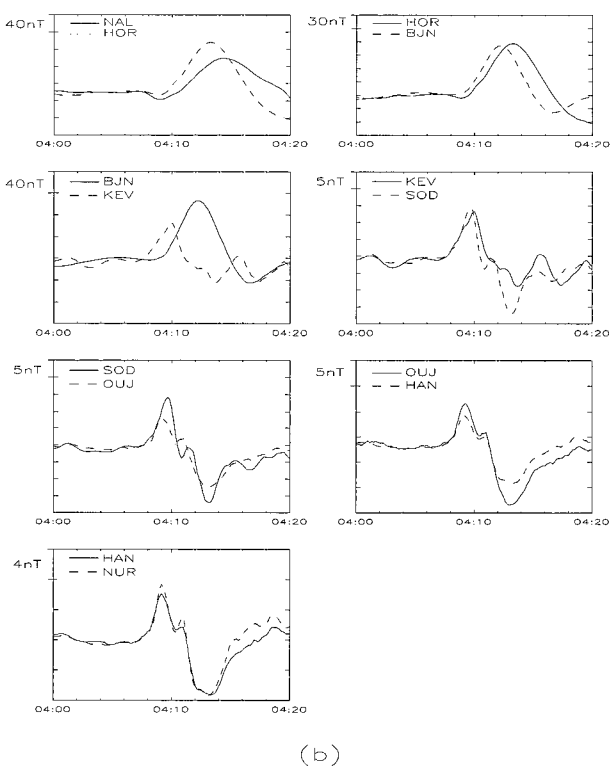

Fig. 8.— Direct comparisons of the magnetic fields observed at the two adjacent stations. Solid line represents the high latitude station and and dashed line represents the low latitude station.

Table 1. Magnetic latitudes and longitudes of the ground stations. The underline represents the stations observed the earliest signal among the each Area.

Network	Station Name	Abbrev.	MLat. (°)	MLon. (°)
IMAGE Area 1	Ny Ålesund	NAL	75.25	112.08
	Hornsund	HOR	74.13	109.59
	Bear Island	BJN	71.45	108.07
	Kevo	KEV	66.32	109.24
	Sodankylä	SOD	63.92	107.26
	Oulujärvi	OUJ	60.99	106.14
	Hankasalmi	HAN	58.71	104.61
	Nurmijärvi	NUR	56.89	102.18
SAMNET Area 2	Hella	HLL	64.49	68.36
	Glenmore	GML	54.91	78.22
	York	YOR	50.93	79.00
210MM Area 3	Zyryanka	ZYK	59.62	216.72
	Magadan	MGD	53.56	218.66
	Moshiri	MSR	37.61	213.23
	Onagawa	ONW	31.65	212.51
GIMA Area 4	Kaktovik	KAK	70.69	257.81
	Arctic	ARC	68.61	259.07
	Ftyukon	FTY	67.29	261.33
	Poker	POK	65.60	260.90
	Gakona	GAK	63.54	265.68
CANOPUS Area 5	Rankin Inlet	RANK	70.37	338.92
	Eskimo Point	ESKI	68.62	336.46
	Fort Churchill	FCHU	66.27	336.68
	Gillam	GILL	63.88	336.20
	Island Lake	ISLL	61.38	336.42
	Pinawa	PINA	57.73	335.08

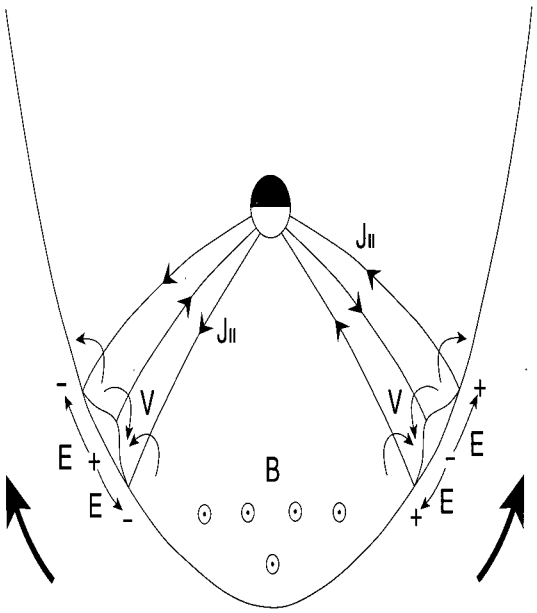

Fig. 9.— Schematic illustration of the effect of compression of the magnetosphere, showing the plasma flows, electric fields, and current systems produced by this interaction.

noon on both the dawn and dusk sides. The magnetic field lines are frozen into this flow, and the resulting motions twist the field lines with the opposite magnetic helicities. Therefore, a downward field-aligned current occurs at dawn and upward at dusk.

From an electrodynamic point of view, the inward and outward flows are accompanied by dawnward and duskward directed azimuthal electric fields, which corresponds to the ideal MHD condition of $\vec{E} + \vec{v} \times \vec{B} = 0$. Thus, the electric field has a positive divergence on the dawn and negative divergence at dusk, and the perturbed region has positive space charge at dawn and negative charge at dusk. These charges discharge along the magnetic field lines, again producing downward currents on the dawn side and upward currents on the dusk side, which is shown in Figure 9.

From the points discussed above, it is possible to clarify a qualitative pattern of observations for the initial signature of SI. At the first impact region, both azimuthal sides would see the opposite field-aligned currents, respectively. The resulting ground magnetic field signature would be caused by the opposite twisting motions, and the transverse magnetic field component would change its polarity from one to another.

IV. SUMMARY

Our study revealed that there is the difference in arrival timing of shock fronts along the dayside magnetic latitude. In the numerical experiment, the compressional components almost simultaneously arrive in the polar region, while the transverse components become differentiated in latitude. In the transverse components, the earliest signals are found near $L = 6$. On the other hand, observation result informs that the first signal was found near 63.5° - 64.5° in magnetic latitude. It corresponds to L = 5.02 - 5.39 in the dipole magnetic field. This observation is consistent with the numerical results. It is that the wavefronts undergo a highly refractive path owing to the plasmasphere and then the arrival timing is differentiated in magnetic latitude. From a mechanical or an eletrodynamical point of view, it is suggested that that the initial signature of SI excites the opposite profile at dawn and dusk, respectively. This feature is very consistent with the ground observations presented in this study. The present analysis of the magnetic field observations during the initial phase of the SI event on September 3, 2000, is based on a case study. Additional observational events will greatly improve our current understanding and allow statistical investigations, which remain as future work.

ACKNOWLEDGEMENTS

This work was supported by the Korea Science & Engineering Foundation grant R14-2002-043-01000-0. We thank all institutes who maintain the IMAGE magnetometer network. Geotail magnetic field data were provided by S. Kokubun through DARTS at the Institute of Space and Astronautical Science (ISAS) in Japan. The authors thank Dr. I.R. Mann and Dr. D.K. Milling for the SAMNET data. SAMNET is a PPARC National Facility deployed and operated by the University of York. The CANOPUS instrument array constructed, maintained and operated by the Canadian Space Agency, provided the data used in this study.

REFERENCES

Araki, T. 1977, Global structure of geomagnetic sudden commencements, Planet. Space Sci., 25, 373

Araki, T. 1994, A physical model of the geomagnetic sudden commencement, in Solar Wind Sources of Magnetospheric Ultra-Low-Frequency Waves, Geophys. Monogr. Ser., ed M. J. Engebretson, K. Takahashi, & M. Scholer, (Washington, D. C. : AGU), 81, pp. 183-200

Araki, T., Fujitani, S., Emoto, M., Yumoto, K., Shiokawa, K., Ichinose, T., Luehr, H., Orr, D., Milling, D. K., Singer, H., Rostoker, G., Tsunomura, S., Yamada, Y.,& Liu, C. F. 1997, Anomalous sudden commencement on March 24, 1991, J. Geophys. Res., 102, 14075

Burlaga, L. F., & Ogilvie, K. W. 1969, Causes of sudden commencements and impulses, J. Geophys. Res., 74, 2815

Chen, L., & Hasegawa, A. 1974, A theory of long-period magnetic pulsations, 1, Steady state excitation of field line resonance, J. Geophys. Res., 79, 1024

Francis, W. E., Green, M. J., & Dessler, A. J. 1959, Hydromagnetic propagation of sudden commencements of magnetic storms, J. Geophys. Res., 64, 1643

Hasegawa, A., Tsui, K. H., & Assis, A. S. 1983, A theory of long-period magnetic pulsations, Geophys. Res. Lett., 10, 765

Hudson, M. K., Kotelnikov, A. D., Li, X., Roth, I., Temerin, M., Wygant, J., Blake, J. B., & Gussenhoven, M. S. 1995, Simulation of proton radiation belt formation during the March 24, 1991 SSC, Geophys. Res. Lett., 22, 291

Hudson, M. K., Elkington, S. R., Lyon, J. G., Marchenko, V. A., Roth, I., Temerin, M., & Gussenhoven, M. S. 1996, MHD/particle simulations of radiation belt formation during a storm sudden commencement, in Radiation Belts: Models and Standards, Geophys. Monogr. Ser., ed Lemaire,J. F., Heynderickx, D., & Baker, D. N. (Washington, D. C. : AGU), 97, pp. 57-62

Kikuchi, T., & Araki, T. 1979a, Transient response of uniform ionosphere and preliminary reverse impulse of geomagnetic storm sudden commencement, J. Atmos. Terr. Phys., 41, 917

Kikuchi, T., & Araki, T. 1979b, Horizontal transmission of the polar electric field to the equator, J. Atmos. Terr. Phys., 41, 927

Knott, K., Pedersen, A., & Wedeken, U. 1985, GEOS 2 electric field observations during a sudden commencement and subsequent substorms, J. Geophys. Res., 90, 1283

Lee, D.-H., & Kim, K. 2000, Propagation of sudden impulses in the magnetosphere: Linear waves, Adv. Space Res., 25(7/8), 1531

Lee, D.-H., & Hudson, M. K. 2001, Numerical studies on the propagation of sudden impulses in the dipole magnetosphere, J. Geophys. Res., 106, 8435

Lee, D.-H., & Lysak, R. L. 1989, Magnetospheric ULF wave coupling in the dipole model: The impulsive excitation, J. Geophys. Res., 94, 17097

Lee, D.-H., & Lysak, R. L. 1999, MHD waves in a three-dimensional dipolar magnetic field: A search for Pi2 pulsations, J. Geophys. Res., 104, 28691

Li, X., Roth, I., Temerin, M., Wygant, J., Hudson, M. K., & Blake, J. B. 1993, Simulation of the prompt energization and transport of radiation belt particles during the March 24, 1991 SSC, Geophys. Res. Lett., 20, 2423

Lysak, R. L., Song, Y., & Lee, D.-H. 1994, Generation of ULF waves by fluctuations in the magnetopause position, in Solar Wind Sources of Magnetospheric Ultra-Low-Frequency Waves, Geophys. Monogr. Ser., ed Engebretson, M. J., Takahashi, K., & Scholer, M. (Washington, D. C. : AGU), 81, pp. 273-281

Nishida, A. 1964, Ionospheric screening effects and sudden commencements, J. Geophys. Res., 69, 1761

Nopper, R. W., Jr., Hughes, W. J., Maclennan, C. G., & McPherron, R. L. 1982, Impulse-excited pulsations during the July 29, 1977, event, J. Geophys. Res., 87, 5911

Petrinec, S. M., K. Yumoto, H. Lühr, D. Orr, D. Milling, K. Hayashi, S. Kokubun, & Araki, T. 1996, The CME event of February 21, 1994: Response of the magnetic field at the Earth's surface, J. Geomagn. Geoelectr., 48, 1341

Stegelmann, E. J., & von Kenschitzki, C. H. 1964, On the interpretation of the sudden commencement of geomagnetic storms, J. Geophys. Res., 69, 139

Tamao, T. 1964, A htdromagnetic interpretation of geomagnetic SSC, Rep. Ionos. Space Res. Jpn., 18, 16

Wedeken, U., Voelker, H., Knott, K., & Lester, M. 1986, SSC-excited pulsations recorded near noon on GEOS 2 and on the ground (CDAW 6), J. Geophys. Res., 91, 3089

Wilken, B., Goertz, C. K., Baker, D. N., Higbie, P. R., & Fritz, T. A. 1982, The SSC on July 29, 1977 and its propagation within the magnetosphere, J. Geophys. Res., 87, 5901

Wilson, C. R., & Sugiura, M. 1961, Hydromagnetic interpretation of sudden commencements of magnetic storms, J. Geophys. Res., 66, 4097